

Supporting Information

Coordinately Unsaturated Single-Fe-Atom with N-Vacancy and Enhanced sp^3 Carbon Defects in Fe-N(sp^2)-C structural unit for Suppression of Cancer Cells Metabolism and Electrochemical Oxygen Evolution

Anubha Yadav^a; Netra Hiremath^b; Bhagirath Saini^d; Babasaheb M. Matsagar^e; Po-Chun Han,^e; Masaki Ujihara^f; Mohammed Hussein Modi^g; Kevin, C.-W. Wu^{eh}; Rakesh K. Sharma^{d}; Raviraj Vankayala^{b,c*}; Saikat Dutta^{a*}*

^aElectrochemical Energy & Sensor Research Laboratory

Amity Institute of Click Chemistry Research & Studies

Amity University

Noida, India

E-mail: sdutta2@amity.edu

^bInterdisciplinary Research Platform Smart Healthcare,

Indian Institute of Technology Jodhpur,

Karwar 342030, Rajasthan, India

^cThe Nanomed Laboratory,

Department of Bioscience & Bioengineering, Indian

Institute of Technology Jodhpur, Karwar 342030, Rajasthan, India.

E-mail: rvankayala@iitj.ac.in

^dSustainable Materials & Catalysis Research Laboratory (SMCRL)

Department of Chemistry

Indian Institute of Technology Jodhpur

Jodhpur, India

E-Mail: rks@iitj.ac.in

^e Department of Chemical Engineering,

National Taiwan University,

Taipei 10617, Taiwan

^f Graduate Institute of Applied Science and Technology,

National Taiwan University of Science and Technology,

Taipei, Taiwan

^g Soft X-ray Applications Lab

Synchrotron Utilization Section

Raja Ramanna Centre for Advanced Technology, Indore, India

^h Department of Chemical Engineering and Materials Science,

Yuan Ze University, Chung-Li,

Taoyuan, Taiwan

S1. Materials and Instrumentation.

All chemicals were purchased from commercial sources and used without further treatment: zinc nitrate hexahydrate ($\text{Zn}(\text{NO}_3)_2 \cdot 6\text{H}_2\text{O}$, Sigma Aldrich, 99%), 2-methylimidazole (Sigma-Aldrich, 99%), cobalt nitrate hexahydrate (Sigma-Aldrich, 99%), nickel nitrate hexahydrate (Sigma-Aldrich, 99%). For hydrosilylation and N-formylation reaction the required chemicals

such as triethyl silane (Spectrochem, India), aniline (Spectrochem, India), 1,4-dioxane (Merk, India) were used without further purification.

Powder X-ray diffraction patterns (PXRD) were collected on a Japan Rigaku Miniflex 600 rotation anode X-ray diffractometer equipped with graphite monochromatized Cu K α radiation ($\lambda = 1.54 \text{ \AA}$). X-ray photoelectron spectroscopy (XPS) measurements were performed by using a NEXSA ThermoFisher Scientific with Al K-alpha source. Field-emission scanning electron microscopy (FE-SEM) was carried out with a field emission scanning electron microanalyzer (FESEM- JEOL 7900F at an acceleration voltage of 5 kV. EXAFS spectroscopy data were collected in Taiwan Light Source Beamlines (nsrrc.org.tw) in a beamline which high resolution DCM X-ray beamline with both collimating and focusing mirrors, which will deliver monochromatic photon beams with energy ranging from 6 keV to 33 keV. The transmission electron microscopy (TEM), high-resolution TEM (HRTEM) and high-angle annular dark-field scanning transmission electron microscopy (HAADF-STEM) images were acquired on JEOL JEM-2100F. EDS was recorded in OXFORD X-MaxN TSR. The nitrogen isotherms were measured by using the automatic volumetric adsorption equipment (Micromeritics ASAP 2020). Prior to gas adsorption/desorption measurement, the samples were dried for 12 h at 433 K under vacuum.

S2. Preparation of Samples.

2. Material and method:

2.1. Synthesis of Fe-phen@ZIF-8

First a mixture of Fe²⁺ (0.5 mmol) and 1,10-phenanthroline (2 mmol) was added to 20 mL ethanol and stirred at 60°C. Then ZIF-8 (900mg) was added to the above-mixed solution and vigorously stirred until all the solvent evaporated. The product was finely ground and named as Fe-Phen@ZIF-8.

Synthesis of Fe/ZIF-8@RF Urea

Resorcinol (15mg), formaldehyde solution (3g), 10 mg urea, and CTAB (15 mg) were first dissolved in 60 ml of deionized water with stirring for 30 min. Then, 200 mg of Fe-Phen@ZIF-8 was dispersed and sonicated for 10 min, followed by stirring for 24 h at room temperature. The resulting precipitate was collected by centrifugation, washed and dried under a vacuum overnight.

2.2. Carbonization of Fe/ZIF-8@RF-Urea

In the first step, high-temperature pyrolysis of Fe/ZIF-8@RF-Urea in a silica crucible was run to access Fe–N–C single atom sites. Fe/ZIF-8@RF-Urea was subjected to heating at 800°C for 30 min under flowing Ar gas to obtain a sample denoted as Fe–N–C-800. Then the Fe–N–C-800 (100mg) were ground with NH₄Cl salts (300mg) thoroughly, followed by elevating the temperature to 950°C in 30 mins to run the pyrolysis for 2h to obtain Fe–SA-950NC. NH₄Cl decomposes to NH₃ and HCl gas at high temperatures, which produce substantial internal stress and etch the carbon, thus creating a multitude of micropores and carbon defects.

MTT assay experiments

The MTT assay is done to evaluate the cell viability of all cells in culture. Cell line NIH3Ts (Murine Fibroblast cell) and A549 (lung cancer cell) were used as cell lines for tumor cell viability analysis. As control, untreated cells were studied. A varied concentration of the Fe-SA materials in 5 different concentration (5, 10, 25, 50, 100, and 200 µg/mL are used. Total 4 replicas of each concentration were tested and best 3 data sets are used.

First, Trypsinize a subconfluent monolayer culture and collect the cells in growth medium containing serum. The suspension was centrifuged for 5 min at 1700 g to pellet the cells. The cells were resuspended in growth medium and counted. The cells were seed in 96-well flat bottom tissue culture plate at a concentration of 10000 cells/200 µl/well. We allowed the cell

to grow and stabilize overnight. Further, cells were treated with different concentrations of Fe-SA prepared in complete medium (in replicates of 4). Next, cells were incubated for 24 h. After treatment with nanomaterial, wash cells with PBS and treated with MTT reagent. Add 5 μ L MTT reagent (conc. 10 mg/ml) and incubate for one and half hrs at 37 °C then remove media and add 100 μ l DMSO to each well. Record absorbance at 570 nm immediately.

Cellular ROS assay

Cell line A549 (Lung cancer cell) and NIH3T3 (fibroblast cells) with control untreated cells. The concentrations of Fe-SA 10 μ g/mL, H₂O₂ 30 μ M and Ascorbic acid 50 mM. First, Trypsinize a subconfluent monolayer culture and collect the cells in growth medium containing serum. The suspension was centrifuged for 5 min at 1700 g to pellet the cells. The cells were resuspended in growth medium and counted. The cells were seeded in 96-well flat bottom tissue culture plate at a concentration of 20000 cells/200 μ l/well. We allowed the cell to grow and stabilize for about 24h. Further, cells were treated with 10 μ g/mL of Fe-SA for 3h. After 3 hours incubation with FeSA, treat the cells either with H₂O₂ or ascorbic acid and incubate the cells with 1h. Wash the cells with PBS and treat the cells with 10 μ M H₂DCF-DA in PBS. Further incubate the cells for 20 min and wash with PBS 2 times. Next, the cells were observed under the fluorescence microscope.

Electrochemical Measurements

The Ni-Foam working electrodes were prepared by homogenous coating ink with a Fe-SA catalyst (40 mg), PVDF (5 mg), conductive carbon black (5 mg) and NMP (500 μ l) onto the nickel foam electrode (1 \times 1 cm²), with the loading of 6 mg/cm². Electrochemical measurements were performed on a CH Instruments (model 660E) with a three-electrode setup, using a coated Nickel foam as the working electrode, Ag/AgCl as the reference electrode and Pt wire as the counter electrode in 1 M KOH. OER activity was measured at a scan rate of 5 mV/s at room

temperature using the LSV technique. The Nernst equation, $E_{RHE} = E_{Ag/AgCl} + 0.199 V + 0.059 \times pH$ was used to convert the potential to a reversible hydrogen electrode (RHE).

Electrochemical impedance spectroscopy (EIS) investigations were performed at onset potential over the frequency range 0.1 Hz to 10^6 Hz. Tafel slope was calculated using polarization curves. The calculation formula was as follows: $\eta = a + b \log j$, where η was the overpotential, j was the current density, and b was the Tafel slope. All of the potentials and voltages are without iR corrected.

Electrochemical Surface Area: The cyclic voltammogram was recorded in the non-faradaic area at various scan rates, and the resulting ECSA was determined. Additionally, the slope of the anodic current density against scan rates graph was used to calculate the electrochemical double layer capacitance (C_{dl}) of the catalytically active surface. The C_{dl} is calculated by using Equation 1

$$i = v C_{dl} \quad (1)$$

where the scan rate is represented by "v" and the measured anodic current density by "i." A straight line with C_{dl} as the slope is generated by plotting i against v . Moreover, ECSA is calculated by dividing the C_{dl} with the specific capacitance (C_s), using a C_s value of $40 \mu F cm^{-2}$.

TOF Calculation: We assume that all moles of catalyst deposited on the electrode is participating in the OER. The TOF values of the FeSA950NC composites coated on the electrodes were determined using Equation 2.

$$TOF = (j \cdot A) / 4 \cdot m \cdot F$$

here, j (20 mA current density); A (surface area of the electrode = $1 cm^{-2}$); m = No. of moles of catalyst deposited on the electrode); F (Faraday efficiency) = $96485 C mol^{-1}$.

$$TOF = \frac{20 \times 10^{-3} A/m^2 \times 1 \times 10^{-4} m^2}{4 \times 2.7 \times 10^{-4} mol \times 96485 C/mol}$$

$$TOF = 0.19 \times 10^{-3} s^{-1}$$

RRDE Experiment:

OER tests were carried out in a 4-electrode system of Autolab RRDE system by using the rotating ring-disk electrode (9RRDE) technique as linear sweep voltammetry (LSV) curves as the OER activity is progressively enhanced in which LSV polarization curves of FeSA950NC at varied rotating speeds (400 to 2000 rpm) was recorded at a varied potentials from (-0.4 to 0.8 V).

EPR Spectral Experiment

Calculation of g-factor:

$$g = h\nu/\beta H \quad (1)$$

where,

$h = 4.135 \times 10^{-15}$ eVs is the Plank constant.

$\nu = 9.48$ GHz is the microwave frequency of X-band spectrometer.

$\beta = 5.788 \times 10^{-5}$ eVT⁻¹ is the electron Bohr magnetron.

H is the applied magnetic Field

Solving equation (1) for electron Bohr magnetron and Plank constant gives,

$$g = 71.4477 \nu \text{ (in GHz)} / B \text{ (in mT)} \quad (2)$$

The EPR test was performed using the X band at 100 k in solid state, the successful insertion of carbon vacancies in the bulk phase of carbon-based materials was demonstrated by the peak signal at the g-value of 2.15 in the EPR pattern of Fe-SA950NC.¹⁻³

Characterization

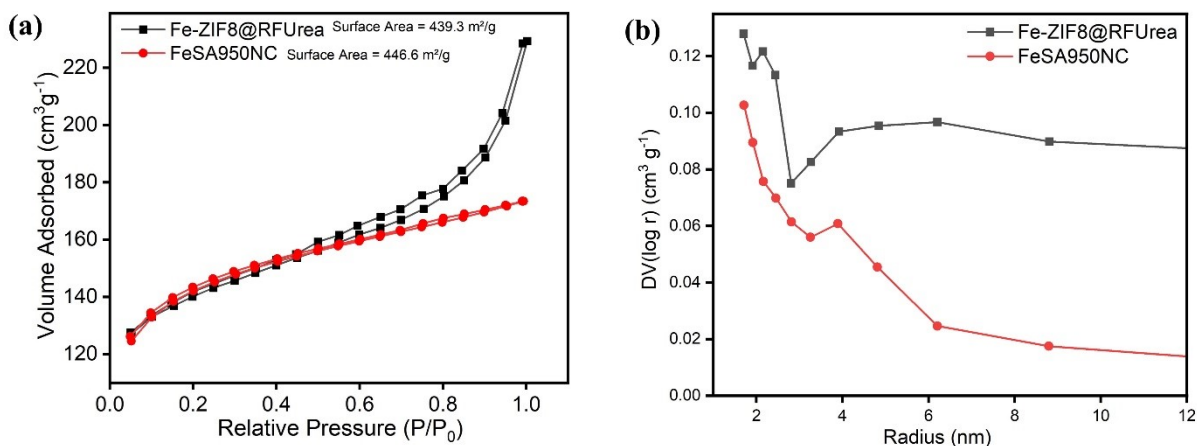


Figure S1. (a) N_2 -adsorption-desorption of Fe-SA950NC as compared to Fe-ZIF-8@RFUrea. (b) Pore-profile analysis of both samples.

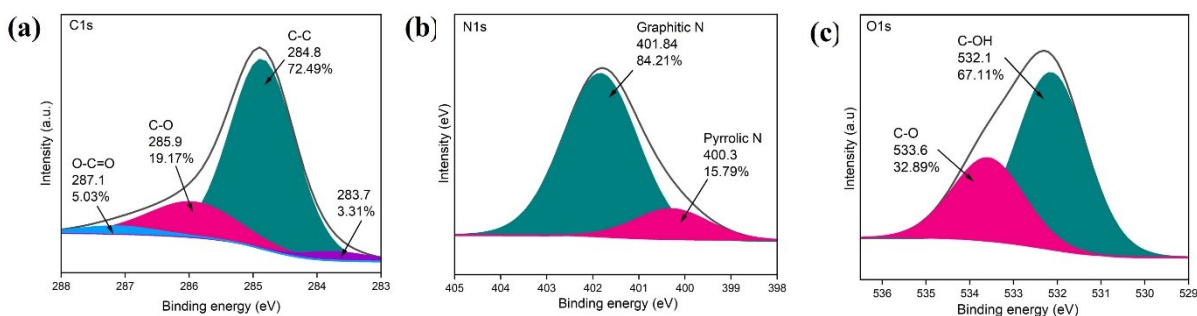


Figure S2. Deconvolution (a) C 1s; (b) N 1s; (c) O 1s spectra of Fe-SA950NC.

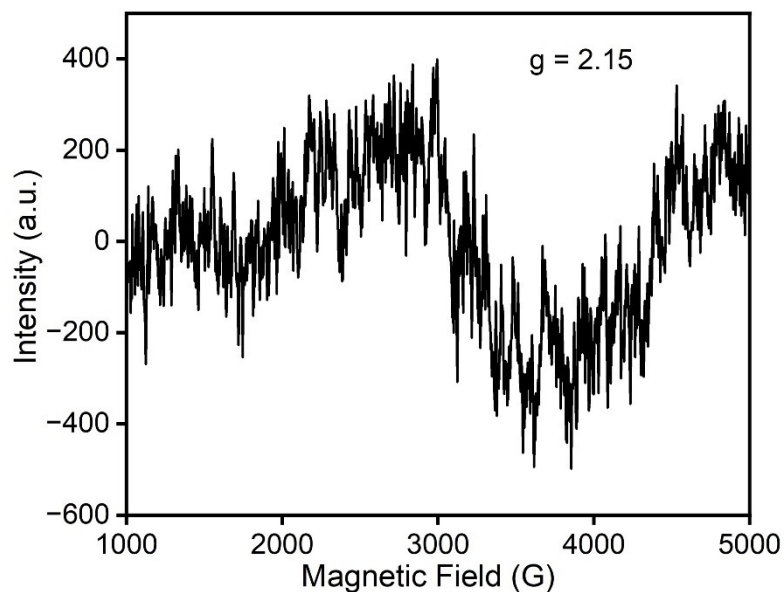


Figure S3. EPR spectra of Fe-SA950NC.

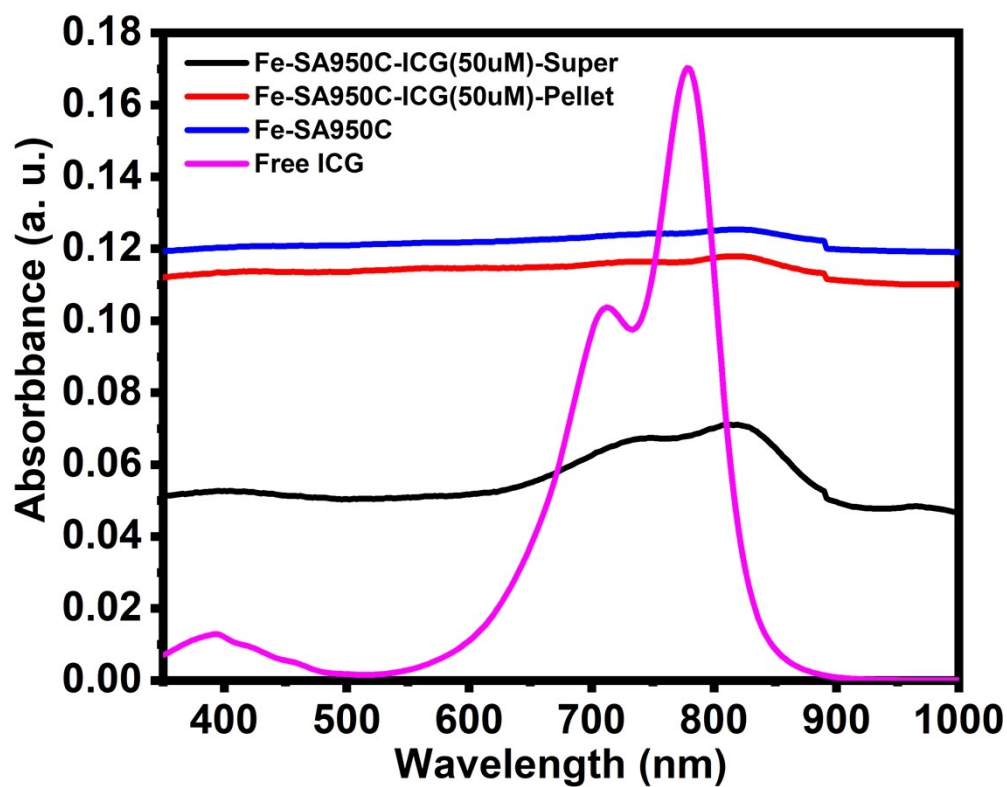


Figure S4. UV-Vis spectrum of Fe-SA950C loaded with ICG.

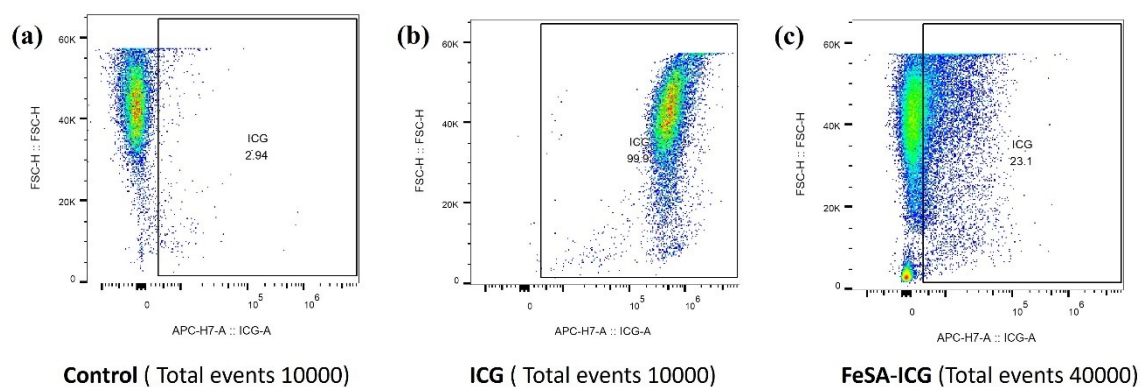


Figure S5. FACS investigation of FeSA-ICG cellular uptake in A549 with control (a), ICG (b), and FeSA-ICG (c).

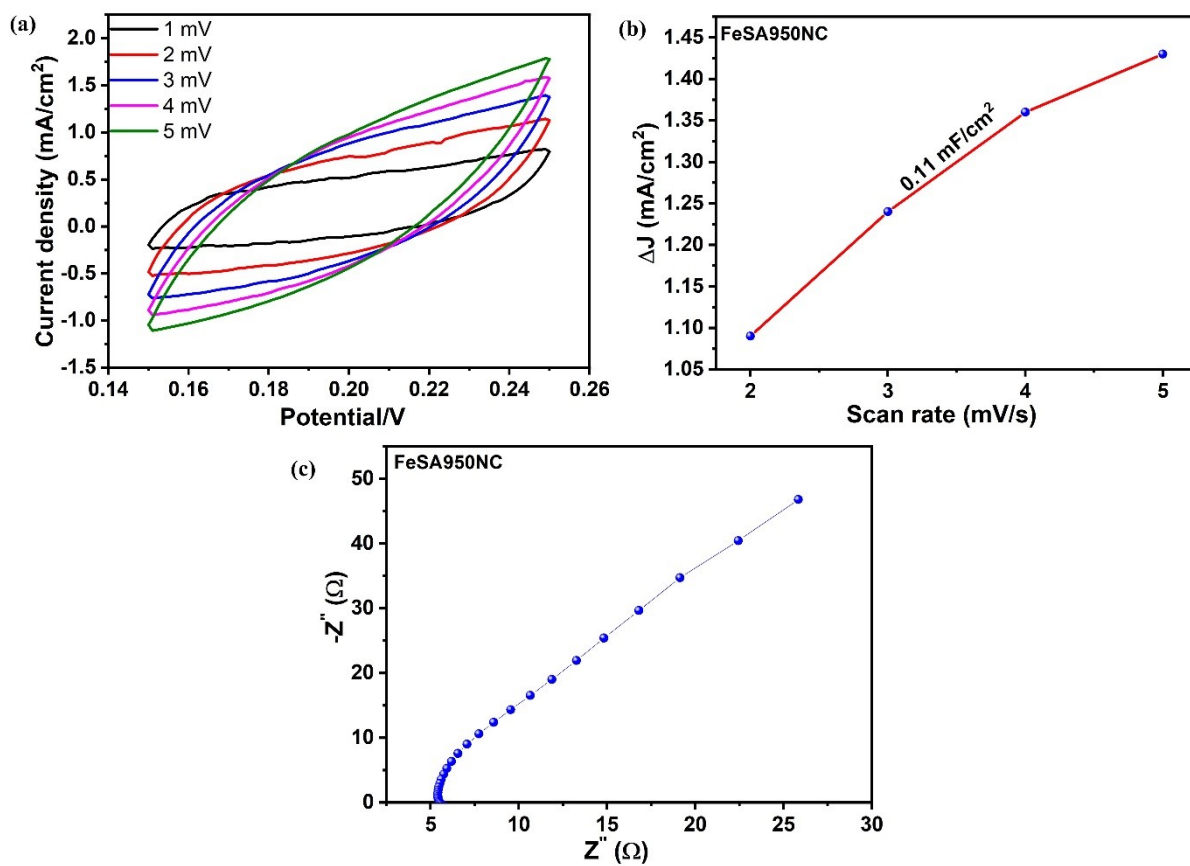


Figure S6. CV curves in non-faradaic region at a scan rate of 1 to 5 mV/s, (b) plot of capacitive current against the scan rate to determine the C_{dl} . (c) Nyquist plot.

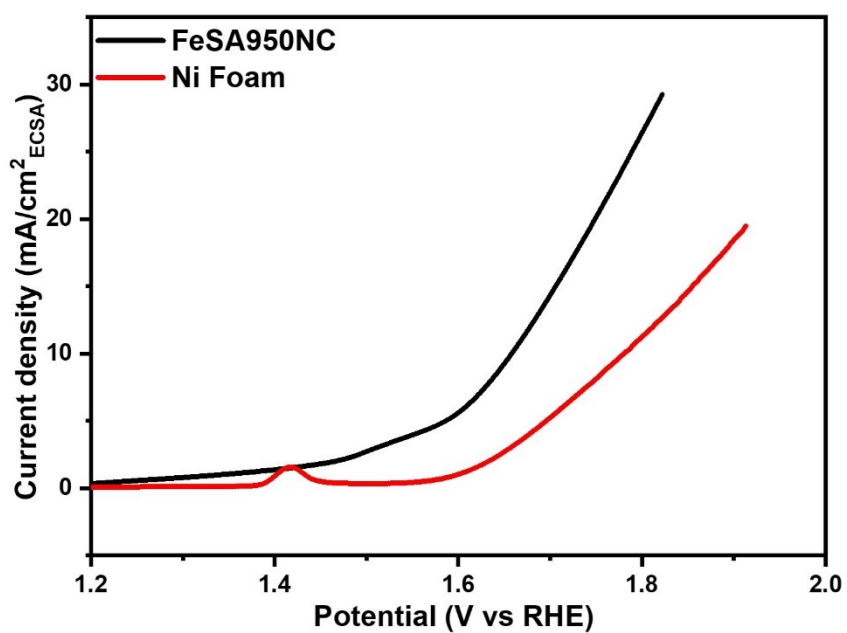


Figure S7. ECSA normalized OER polarization curve of FeSA950-NC and Ni Foam.

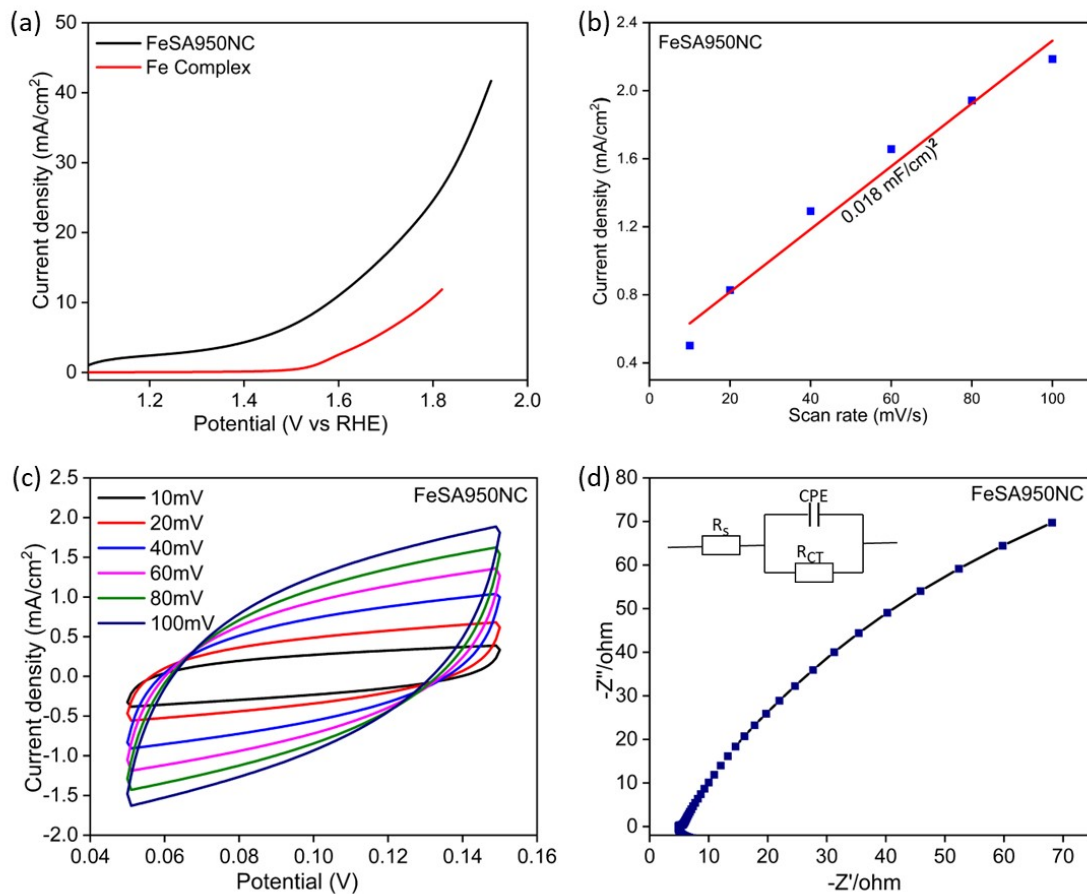


Figure S8. OER performance of FeSA950NC/CC and Fe-complex electrocatalyst. (a) polarization curves at 5 mV/s in 1M KOH for FeSA950NC and Fe-1,10-phenanthroline complex. (b) Plot of capacitive current against the scan rate to determine the C_{dl} . (c) non-faradic cyclic voltammetry at different scan rates from 10 to 100mV. (d) Nyquist plot.

1. R-space FT-EXAFS fitting analysis.

Table S1. Structural parameters of FeSA950NC extracted from the EXAFS fitting. ($S_0^2=3.344$).

Scattering Pair	CN	R(Å)	σ^2	ΔE_0 (eV)	R factor
Fe-N	2	0.0155448	0.00497	-3.267	2.00912

S_0^2 is the amplitude reduction factor; CN is the coordination number; R is interatomic distance (the bond length between central atoms and surrounding coordination atoms); σ^2 is Debye-Waller factor (a measure of thermal and static disorder in absorber-scatterer distances); ΔE_0 is edge-energy shift (the difference between the zero kinetic energy value of the sample and that of the theoretical model). R factor is used to value the goodness of the fitting.

Table S2. The comparison of oxygen evolution reaction activity of recently reported Fe-N-C single atom catalysts.

S.No	Electrocatalyst	Electrolyte	Current density (mA/cm ²)	Overpotential (mV)	Reference
1.	Fe-N _x -C		10	600	4
2.	S,N-Fe/N/C-CNT	0.1M KOH	10	370	5
3.	P/Fe-N-C	1 M NaOH	10	304	6
4.	P/Fe@NC	1 M NaOH	10	384	6
5.	Fe-N-C	1 M NaOH	10	450	6
6.	Fe-N-C/rGO	0.1 M KOH	10	360	7

7.	Fe/N-G-SAC	0.1 M KOH	10	370	8
8.	Fe-SNC@ 900	0.1 M KOH	10	402	9
9.	Fe SAs/NC	0.1 M KOH	10	320	10
10	Fe ₁ (OH) _x /P-C	1 M KOH	10	320	11
11	Fe-UTN	1 M KOH	10	270	12
12	Fe-N-900	1 M KOH	10	380	13
13	Fe ₃ C/Fe-N-C	1 M KOH	10	338	14
14	Commercial IrO ₂	1M KOH	10	270	6
15	FeSA950NC	1 M KOH	10	210	This study

References

1. L. Shan, Y. Ma, S. Xu, M. Zhou, M. He, A. M. Sheveleva, R. Cai, D. Lee, Y. Cheng, B. Tang, B. Han, Y. Chen, L. An, T. Zhou, M. Wilding, A. S. Eggeman, F. Tuna, E. J. L. McInnes, S. J. Day, S. P. Thompson, S. J. Haigh, X. Kang, B. Han, M. Schröder and S. Yang, *Communications Materials*, 2024, **5**, 104.
2. H. Tian, A. Song, P. Zhang, K. Sun, J. Wang, B. Sun, Q. Fan, G. Shao, C. Chen, H. Liu, Y. Li and G. Wang, *Adv. Mater.*, 2023, **35**, 2210714.
3. Y. Zhang, G. Li, J. Wang, D. Luo, Z. Sun, Y. Zhao, A. Yu, X. Wang and Z. Chen, *Adv. Energy Mater.*, 2021, **11**, 2100497.
4. J. Han, X. Meng, L. Lu, J. Bian, Z. Li and C. Sun, *Advanced Functional Materials*, 2019, **29**, 1808872.
5. P. Chen, T. Zhou, L. Xing, K. Xu, Y. Tong, H. Xie, L. Zhang, W. Yan, W. Chu, C. Wu and Y. Xie, *Angewandte Chemie International Edition*, 2017, **56**, 610-614.
6. Y. Zhou, R. Lu, X. Tao, Z. Qiu, G. Chen, J. Yang, Y. Zhao, X. Feng and K. Mullen, *J Am Chem Soc*, 2023, **145**, 3647-3655.
7. L. Li, Y.-J. Chen, H.-R. Xing, N. Li, J.-W. Xia, X.-Y. Qian, H. Xu, W.-Z. Li, F.-X. Yin, G.-Y. He and H.-Q. Chen, *Nano Research*, 2022, **15**, 8056-8064.
8. M. Xiao, Z. Xing, Z. Jin, C. Liu, J. Ge, J. Zhu, Y. Wang, X. Zhao and Z. Chen, *Advanced Materials*, 2020, **32**, 2004900.
9. Z. Chen, X. Peng, Z. Chen, T. Li, R. Zou, G. Shi, Y. Huang, P. Cui, J. Yu, Y. Chen, X. Chi, K. P. Loh, Z. Liu, X. Li, L. Zhong and J. Lu, *Adv. Mater.*, 2023, **35**, 2209948.
10. Z. Li, S. Ji, C. Xu, L. Leng, H. Liu, J. H. Horton, L. Du, J. Gao, C. He, X. Qi, Q. Xu and J. Zhu, *Adv. Mater.*, 2023, **35**, e2209644.
11. Z. Zhang, C. Feng, X. Li, C. Liu, D. Wang, R. Si, J. Yang, S. Zhou and J. Zeng, *Nano Lett*, 2021, **21**, 4795-4801.

12. G. Shen, R. Zhang, L. Pan, F. Hou, Y. Zhao, Z. Shen, W. Mi, C. Shi, Q. Wang, X. Zhang and J. J. Zou, *Angew Chem Int Ed Engl*, 2020, **59**, 2313-2317.
13. D. Lyu, Y. B. Mollamahale, S. Huang, P. Zhu, X. Zhang, Y. Du, S. Wang, M. Qing, Z. Q. Tian and P. K. Shen, *J. Catal.*, 2018, **368**, 279-290.
14. Y. Chen, X. Kong, Y. Wang, H. Ye, J. Gao, Y. Qiu, S. Wang, W. Zhao, Y. Wang, J. Zhou and Q. Yuan, *Chem. Eng. J.*, 2023, **454**, 140512.